Journal of Organometallic Chemistry, 202 (1980) 329—339
Elsevier Sequoia S.A., Lausanne — Printed in The Netherlands

SYNTHESIS AND STRUCTURAL CHARACTERIZATION OF THE $[NiRh_6(CO)_{16}]^{2-}$ DIANION: A NEW MIXED HEPTANUCLEAR CARBONYL CLUSTER. EVIDENCE FOR OTHER Ni—Rh MIXED CARBONYL CLUSTER ANIONS

ALESSANDRO FUMAGALLI *, GIULIANO LONGONI, PAOLO CHINI
Istituto di Chimica Generale dell'Università e Centro del CNR, Via G. Venezian 21, 20133 Milano (Italy)

ALBERTO ALBINATI and SERGIO BRÜCKNER
Istituto di Chimica Generale del Politecnico, Piazza Leonardo da Vinci 32, 20133 Milano (Italy)

(Received June 5th, 1980)

Summary

The first heptanuclear mixed carbonyl cluster, the anion $[NiRh_6(CO)_{16}]^{2-}$, has been prepared by redox condensation of $[Rh_6(CO)_{15}]^{2-}$ with $[Ni_6(CO)_{12}]^{2-}$ or $Ni(CO)_4$. The structure of the metallic framework is based on a distorted octahedron of Rh atoms capped on one face by a nickel atom and is closely related to that previously observed in the isoelectronic $[Rh_7(CO)_{16}]^{3-}$ anion. Evidence is also reported for the existence of $[NiRh_5(CO)_{15}]^-$ and $[NiRh_4(CO)_{12}]^{2-}$.

Results and discussion

(a) Synthesis of $[NiRh_6(CO)_{16}]^{2-}$

After characterizing some mixed Pt—Rh clusters [1], we have extended our investigation to mixed Ni—Rh carbonyl systems. Because of the general instability of nickel clusters toward decomposition by carbon monoxide, leading to formation of $Ni(CO)_4$ [2], the approach had to be limited to synthetic routes employing a nitrogen atmosphere and preformed carbonyl species of nickel and rhodium.

Reaction of $[Rh_6(CO)_{15}]^{2-}$ salts ($[N(n\text{-}Bu)_4]^+$ or $[PPN]^+$) [3] with $[Ni_6(CO)_{12}]^{2-}$ salts ($[NMe_4]^+$ or $[NEt_4]^+$) [4] in THF under nitrogen gives an almost pure solution of the $[NiRh_6(CO)_{16}]^{2-}$ dianion, because the $[Rh_7(CO)_{16}]^{3-}$ [3—5] anion, which is formed as a by-product, separates as an insoluble precipi-

0022—328X/80/0000—0000/$02.25,

tate. The most probable stoichiometry is:

$$19[Rh_6(CO)_{15}]^{2-} + 2[Ni_6(CO)_{12}]^{2-} \xrightarrow{N_2} 12[NiRh_6(CO)_{16}]^{2-} + 6[Rh_7(CO)_{16}]^{3-} + 21\ CO \quad (1)$$

This reaction is remarkable because it proceeds in the presence of an excess of either of the reagents, the excess remaining unchanged. Treatment of the solution with isopropanol and an excess of $[N(n\text{-}Bu)_4]Cl$ or [PPN]Cl, followed by subsequent recrystallization gives well formed black crystals in the shape of hexagonal prisms. The crystalline product is stable for some time in the air, but is oxidized in solution within a few seconds. In solution the product is also unstable towards carbon monoxide since it is quickly decomposed in a process representing the back reaction of the following equilibrium:

$$[Rh_6(CO)_{15}]^{2-} + Ni(CO)_4 \underset{CO}{\overset{N_2}{\rightleftharpoons}} [NiRh_6(CO)_{16}]^{2-} + 3\ CO \quad (2)$$

This equilibrium also provides the most convenient way of producing the mixed anion: e.g. the reaction between $[Rh_6(CO)_{15}]^{2-}$ and excess $Ni(CO)_4$ under nitrogen. It is worth noting that the analogous equilibrium [3]:

$$[Rh_6(CO)_{15}]^{2-} + [Rh(CO)_4]^- \underset{-70\,^\circ C\ CO}{\overset{25\,^\circ C\ N_2}{\rightleftharpoons}} [Rh_7(CO)_{16}]^{3-} + 3\ CO \quad (3)$$

lies to the left only at low temperature.

Probably, in the decomposition of the Ni—Rh mixed metal species, it is the large energy of the Ni—C bonds which provides the driving force to make the reaction possible at room temperature.

The infrared absorptions of the $[NiRh_6(CO)_{16}]^{2-}$ anion in the carbonyl stretching region are slightly different for the NBu_4^+ and PPN salts, probably because of the presence of ion pairs; ν(CO)(THF soln, ± 5 cm^{-1}): NBu_4: 2030vw, 1985s(br), 1850m (br), 1800ms, 1785ms, 1770ms; PPN: 2030vw, 1980s (br), 1845m (br), 1800ms (sharp), 1770ms (br). The shape of the IR bands (Fig. 1) is quite similar to that observed in the isostructural $[Rh_7(CO)_{16}]^{3-}$ anion, but with a shift to higher frequencies of about 30 cm^{-1} due to the smaller negative charge and consequent reduced back-donation. The green-yellow color is also reminiscent of that of $[Rh_7(CO)_{16}]^{3-}$.

(b) Evidence for other mixed metal species

Other mixed Ni—Rh carbonyl anions have been observed but not yet analytically and structurally characterized. For instance, a species formulated as $[NiRh_5(CO)_{15}]^-$ is the main product of a reaction with the proposed stoichiometry [4]:

$$\tfrac{1}{2}[Ni_5(CO)_{12}]^{2-} + \tfrac{5}{4}Rh_4(CO)_{12} \xrightarrow[N_2]{i\text{-}PrOH} [NiRh_5(CO)_{15}] + \tfrac{3}{2}Ni(CO)_4 \quad (4)$$

The IR spectrum of the isolated brown powder in THF (ν(CO) = 2025s, 2010m, 1780ms cm^{-1}) is quite similar to that of the known $[PtRh_5(CO)_{15}]^-$ [1]. Attempts to obtain an analytically pure crystalline product by slow diffusion

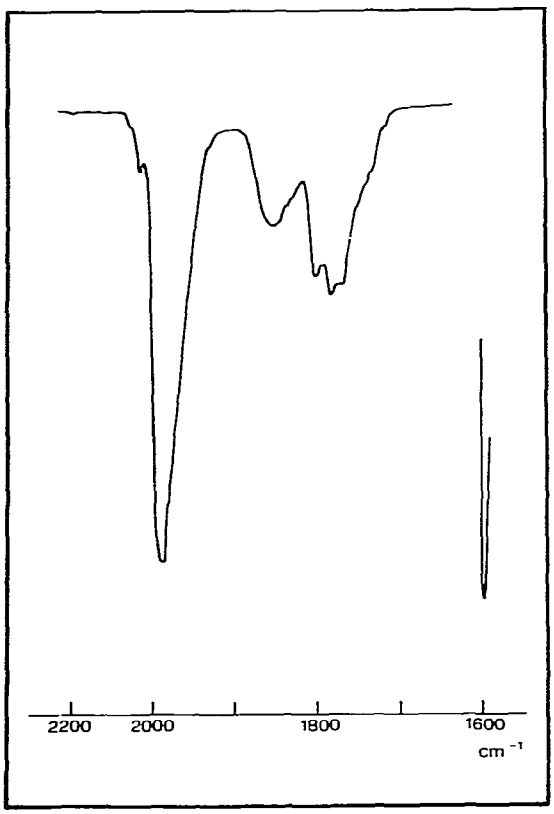

Fig. 1. IR spectrum of $[N(n\text{-}Bu)_4]_2[NiRh_6(CO)_{16}]$ in THF solution.

techniques failed, leading after a week both to unknown decomposition products and some $Ni(CO)_4$.

Treatment of a THF solution of the brown anion with CO, however, immediately resulted in decomposition according to the simple scheme:

$$[NiRh_5(CO)_{15}]^- + 4\ CO \xrightarrow[\text{room temp.}]{\text{CO, 1 atm.}} Ni(CO)_4 + [Rh_5(CO)_{15}]^- \qquad (5)$$

This facile formation of the recently characterized $[Rh_5(CO)_{15}]^-$ anion [6] supports our formulation of the mixed metal precursor as $[NiRh_5(CO)_{15}]^-$.

Reaction of excess $Ni(CO)_4$ with $[Rh_4(CO)_{11}]^{2-}$ [7] takes a different course and the THF solution now becomes yellow-orange. The IR spectrum shows a rather complicated pattern due to several bands. Upon evacuation, however, the color changes to red-brown and the IR spectrum becomes simpler (ν(CO) = 1980s, 1945ms, 1810m cm^{-1}). The shapes and positions of these latter bands are quite reminiscent of those found in $[PtRh_4(CO)_{12}]^{2-}$ [8]. Treatment of the product (isolated as the $[PPN]^+$ salt in a microcrystalline state) with CO in THF solution gave immediate decomposition leading to the starting materials $Ni(CO)_4$ and $[Rh_4(CO)_{11}]^{2-}$ (IR evidence).

Upon further standing $[Rh(CO)_4]^-$ and $[Rh_6(CO)_{15}]^{2-}$ appeared, in accord with

the known CO induced disproportionation of the $[Rh_4(CO)_{11}]^{2-}$ dianion [7].

In the light of the results above, we suggest that the first step in the condensation must lead to an unstable intermediate: possibly a $[NiRh_4(CO)_{14}]^{2-}$ species (some bands in the initial IR spectrum agree fairly well with those the known $[PtRh_4(CO)_{14}]^{2-}$) [8]. On evacuation CO would be released to give the more stable species $[NiRh_4(CO)_{12}]^{2-}$. This overall process can be written in terms of consecutive equilibria:

$$Ni(CO)_4 + [Rh_4(CO)_{11}]^{2-} \underset{CO}{\overset{N_2}{\rightleftharpoons}} [NiRh_4(CO)_{14}]^{2-} \underset{CO}{\overset{N_2}{\rightleftharpoons}} [NiRh_4(CO)_{12}]^{2-} \qquad (6)$$

Further work is in progress in order to isolate these two mixed anions in a crystalline form suitable for X-ray structural determination.

(c) Description of the structure in $[NiRh_6(CO)_7(\mu_2\text{—}CO)_6(\mu_3\text{—}CO)_3]^{2-}$

The metal cluster framework of the anion is a distorted octahedron of Rh atoms capped on a face by a Ni atom; a geometry similar to that found in the

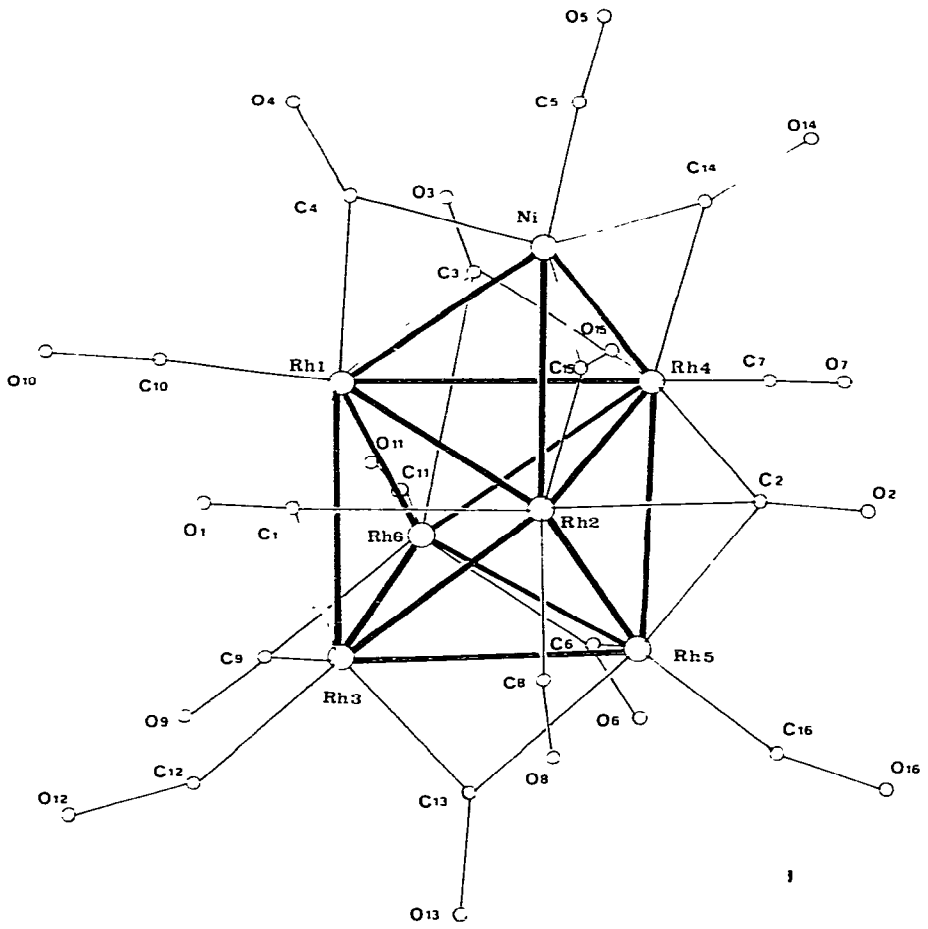

Fig. 2. A perspective view of the $[NiRh_6(CO)_{16}]^{2-}$ dianion.

isoelectronic and isostructural compound $[Rh_7(CO)_{16}]^{3-}$ [5]. A perspective view of the molecule is shown in Fig. 2.

The average bond distance between the two staggered triangular layers defined by atoms Rh(1), Rh(2), Rh(4) and Rh(3), Rh(5), Rh(6) (2.782(5) ± 0.019 Å) * is significantly longer than the other intertriangular distances (2.761(5) ± 0.003 and 2.716(5) ± 0.010 Å, respectively) giving rise to a trigonal antiprismatic distortion of the idealized metallic octahedron.

A further distortion is introduced in the trigonal antiprism by the non-equivalence of the interlayer Rh—Rh distances (values in the range 2.754(5)—2.798(5) Å) in such a way that the top and the bottom faces are no longer parallel.

Finally the capping Ni atom is at non-equivalent bonding distances from the Rh atoms: more precisely, two shorter bonds of average value 2.643(5) Å and a longer one of 2.798(5) Å: these two values may be compared with 2.73(1) and 2.81(1) Å found in the analogous deformation of the $[Rh_7(CO)_{16}]^{3-}$ [5].

The trigonal antiprismatic distortion of the Rh atom octahedron can be easily accounted for by the presence of the Ni atom capping the top triangular face and of the three bridging carbonyls in the bottom face.

The carbonyl arrangement is also similar to that found in $[Rh_7(CO)_{16}]^{3-}$: one terminal CO is bound to each metal atom, three CO are edge-bridging the Ni—Rh bonds while three span the bonds of the bottom triangular face (Rh(3), Rh(5), Rh(6)); finally three more CO molecules are alternately triply bridging on three of the six remaining faces of the antiprism, i.e., (Rh(1)—Rh(2)—Rh(3)), (Rh(1)—Rh(4)—Rh(6)) and (Rh(2)—Rh(4)—Rh(5)). The average metal to carbon bond lengths for the terminal, double and triply bridging CO are 1.76(5) ± 0.1, 1.95(5) ± 0.06, 2.19(5) ± 0.08 Å, respectively.

The final Fourier difference maps show a clear indication of a disordered situation for the O(12) and O(16) atoms between two different orientations, which results in apparently unusual M—C—O bond angles (145.0(8)° and 146.2(8)°, respectively).

It is noteworthy that the metal—carbon bonds of the carbonyls edge-bridging between Ni and Rh should be different in view of the smaller metallic radius of the Ni atom (0.1 Å less than Rh); however, we found for this compound values equal within one e.s.d. (av. Ni—C 1.98 ± 0.06 and Rh—C 1.94 ± 0.05 Å), which can be taken as an indication of asymmetric bridging. Moreover there is a significant deviation from a symmetric situation for the triply bridging CO ligands (av. Rh—C 2.14 and 2.28 Å, respectively), the longer distance being associated with the Rh atoms of the bottom plane; both these effects may reflect an electron transfer from the Ni to Rh atoms, as expected from the difference in electronegativity between these two atomic species.

The two crystallographically independent tetrabutylammonium cations show the expected geometry with average bond lengths of 1.45(7) Å for C—N and 1.53(9) Å for C—C.

* ± values refer to the spread of the values, while e.s.d.'s are given in parentheses.

TABLE 1

ATOMIC COORDINATES AND THERMAL PARAMETERS FOR THE ANION $[NiRh_6(CO)_{16}]^{2-}$
(e.s.d.'s on the last significant figure are given in parentheses: anisotropic temperature factors in the form: $T = \exp -\frac{1}{4}(B_{11}a^{*2}h^2 + B_{22}b^{*2}k^2 + B_{33}c^{*2}l^2 + 2B_{12}a^*b^*hk + 2B_{13}a^*c^*hl + 2B_{23}b^*c^*kl)$.

	x/a	y/b	z/c	B_{11}	B_{22}	B_{33}	B_{12}	B_{13}	B_{23}
Rh(1)	0.3346(1)	0.0136(2)	0.2347(2)	6.6(2)	6.3(2)	5.8(2)	0.5(1)	−0.5(1)	−0.3(1)
Rh(2)	0.3928(1)	−0.0762(2)	0.2713(2)	8.0(2)	7.3(2)	6.3(2)	0.7(2)	1.9(2)	0.6(2)
Rh(3)	0.3976(1)	0.0140(2)	0.1502(2)	6.6(2)	6.9(2)	5.6(1)	0.2(2)	−0.5(1)	−0.2(1)
Rh(4)	0.3773(1)	0.0469(2)	0.3525(2)	5.9(2)	8.4(2)	8.4(2)	0.3(1)	0.2(1)	2.1(2)
Rh(5)	0.4392(1)	0.0462(2)	0.2678(2)	7.5(2)	6.2(2)	6.9(2)	1.4(1)	1.3(2)	0.8(2)
Rh(6)	0.3822(1)	0.1341(2)	0.2314(2)	7.2(2)	6.0(2)	7.0(2)	0.1(2)	−0.6(2)	0.8(2)
Ni	0.3332(2)	−0.0680(3)	0.3520(3)	7.1(3)	8.6(4)	7.0(3)	−0.4(3)	1.0(3)	1.5(3)

	x/a	y/b	z/c	B_{iso}(Å^2)
O(1)	0.3452(8)	−0.1268(15)	0.1443(15)	9.4(8)
O(2)	0.4387(7)	−0.0518(15)	0.4063(14)	8.3(7)
O(3)	0.3099(7)	0.1436(15)	0.3242(14)	8.2(7)
O(4)	0.2650(10)	−0.0450(18)	0.2878(20)	9.6(9)
O(5)	0.2900(9)	−0.1480(21)	0.4453(20)	10.8(1.0)
O(6)	0.4539(8)	0.2001(17)	0.2481(16)	10.2(9)
O(7)	0.4050(9)	0.1766(21)	0.4334(20)	10.6(1.0)
O(8)	0.4526(10)	−0.1680(20)	0.2147(19)	10.5(1.1)
O(9)	0.3920(8)	0.1589(17)	0.0751(17)	10.7(9)

O(10)	0.2911(8)	0.0705(18)	0.1086(17)	10.5(9)
O(11)	0.3602(11)	0.2903(22)	0.2248(22)	11.3(1.2)
O(12)	0.3991(10)	−0.0384(21)	0.0011(21)	15.2(1.0)
O(13)	0.4762(9)	0.0256(20)	0.1300(19)	10.3(1.1)
O(14)	0.3440(11)	0.0034(22)	0.4891(22)	10.6(1.2)
O(15)	0.3675(9)	−0.2123(19)	0.3418(18)	11.4(9)
O(16)	0.5051(10)	0.0647(20)	0.3311(22)	15.1(1.1)
C(1)	0.3584(12)	−0.0811(26)	0.1797(25)	8.4(1.2)
C(2)	0.4223(10)	−0.0262(20)	0.3567(24)	7.1(9)
C(3)	0.3326(11)	0.1071(22)	0.3055(23)	7.4(1.2)
C(4)	0.2951(13)	−0.0364(26)	0.2848(26)	9.4(1.3)
C(5)	0.3065(17)	−0.1166(34)	0.4025(33)	12.9(1.2)
C(6)	0.4328(12)	0.1447(25)	0.2474(23)	8.9(1.1)
C(7)	0.3971(14)	0.1259(28)	0.4013(28)	11.2(1.4)
C(8)	0.4313(14)	−0.1245(29)	0.2383(28)	11.6(1.5)
C(9)	0.3902(14)	0.1187(29)	0.1252(29)	10.9(1.2)
C(10)	0.3082(11)	0.0507(23)	0.1567(22)	7.8(9)
C(11)	0.3696(14)	0.2246(29)	0.2276(29)	11.1(1.3)
C(12)	0.4096(16)	−0.0270(34)	0.0589(32)	14.3(1.2)
C(13)	0.4498(10)	0.0263(32)	0.1659(33)	12.2(1.0)
C(14)	0.3467(15)	0.0027(32)	0.4269(31)	12.6(1.1)
C(15)	0.3674(11)	−0.1518(24)	0.3229(23)	8.1(9)
C(16)	0.4814(17)	0.0414(34)	0.2910(35)	15.9(1.3)

Experimental

All the synthetic work was carried out under N_2 unless otherwise stated, using solvents distilled and stored under N_2. All the starting carbonyl compounds except $Ni(CO)_4$, were prepared accordingly to literature methods. IR spectra were recorded on a Perkin-Elmer 457 spectrophotometer and the reported analyses were performed on the metals by atomic absorption and, on the cation, by gravimetric determination as the $[B(C_6H_5)_4]^-$ salt, after mineralization with Cl_2 and conc. HCl.

$[NiRh_6(CO)_{16}]^{2-}$ as $[N(n\text{-}Bu)_4]^+$ and $[PPN]^+$ salts

(a) From $[Rh_6(CO)_{15}]^{2-}$ and $Ni(CO)_4$. 150 mg of $[N(n\text{-}Bu)_4]_2[Rh_6(CO)_{15}]$ (0.1 mmol) in 10 ml THF, are treated with 1.0 ml of $Ni(CO)_4$ 0.2—0.3 *M* in THF. After 3 hours stirring, if any precipitate is present the solution is filtered and then evacuated to dryness to remove the excess of $Ni(CO)_4$. The residue is treated again with THF (about 5 ml) and by slow diffusion of i-PrOH (20 ml) to give black crystals (yield up to 90%).

To obtain the $[PPN]^+$ salt the reaction is carried out up to the filtration step described above and then [PPN]Cl in i-PrOH (0.6 g/10 ml) is added: a further 20 ml of i-PrOH leads to almost quantitative recover of the product. The product is filtered off, washed with i-PrOH (10 ml in two portions) and vacuum dried. The recrystallization from THF/1-PrOH by slow diffusion gives black crystals (yield 190 mg). Analysis, found: Rh, 30.07; Ni, 2.98; PPN, 44.92. $C_{88}H_{60}N_2NiO_{16}P_4Rh_6$ calcd.: Rh, 28.05; Ni, 2.66; PPN, 48.93%.

(b) From $[Rh_6(CO)_{15}]^{2-}$ and $[Ni_6(CO)_{12}]^{2-}$. In a typical preparation 100—150 mg of $[Rh_6(CO)_{15}]^{2-}$, as the $[PPN]^+$ or $[N(n\text{-}Bu)_4]^+$ salt, (0.05—0.1 mmol) are reacted in THF (10 ml) with excess $[Ni_6(CO)_{12}]^{2-}$ as the $[NMe_4]^+$ or $[NEt_4]^+$ salt (20—30 mg; 0.02—0.04 mmol); after 3 hours the greenish solution obtained upon stirring is filtered from the $[Rh_7(CO)_{16}]^{3-}$ precipitated, and excess [N-(n-Bu)$_4$]Br or [PPN]Cl in i-PrOH is added; some water can help in recovering the product which is filtered off and washed with water and then i-PrOH. The greenish-brown powder is vacuum dried. The product is treated with some THF (about 5 ml) and some insoluble material is filtered off. By slow diffusion of i-PrOH (20 ml) a crystalline product is obtained (yield 0.3—0.5 mol per mol of starting $[Rh_6(CO)_{15}]^{2-}$).

Crystallographic data collection of $[N(n\text{-}Bu)_4]_2[NiRh_6(CO)_{16}]$

$NiRh_6C_{48}O_{16}N_2H_{72}$: mol. wt. = 1608.67, orthorhombic, D_c = 1.728 g cm^{-3}. From systematic absences the space group was uniquely determined as *Pbca* (No. 61) with $Z = 8$. The black crystals are unstable in the air. Data were collected on a prismatic crystal (of approximate dimensions 0.3 × 0.4 × 0.5 mm) sealed in a Lyndemann capillary under N_2. The cell constants a = 36.502(12), b = 18.181(6), c = 18.626(6) Å, were obtained from a least square fit of the 2θ values of 25 diffractometer centered reflections. Data were collected using a Philips four circle automated diffractometer up to $\sin\theta/\lambda$ = 0.5271 Å^{-1} (Mo-$\bar{K}_\alpha$ radiation, graphite monochromated, λ = 0.71069) using an $\omega/2\theta$ scan technique.

The scan speed used was 0.04° s^{-1} with a scan width of 1.20°; two background

TABLE 2

BOND LENGTHS (Å)

(e.s.d.'s on the last significant digit are given in parentheses)

Ni—Rh(1)	2.643(7)	Rh(1)—C(1)	2.18(5)
Ni—Rh(2)	2.648(7)	Rh(1)—C(3)	2.15(5)
Ni—Rh(4)	2.638(7)	Rh(2)—C(1)	2.12(5)
Rh(1)—Rh(2)	2.765(5)	Rh(2)—C(2)	2.12(5)
Rh(1)—Rh(3)	2.785(5)	Rh(3)—C(1)	2.31(5)
Rh(1)—Rh(4)	2.760(5)	Rh(4)—C(3)	2.15(5)
Rh(1)—Rh(6)	2.798(5)	Rh(4)—C(2)	2.11(5)
Rh(2)—Rh(3)	2.794(5)	Rh(5)—C(2)	2.20(5)
Rh(2)—Rh(4)	2.759(5)	Rh(6)—C(3)	2.33(5)
Rh(2)—Rh(5)	2.796(5)		
Rh(3)—Rh(5)	2.727(5)		
Rh(3)—Rh(6)	2.714(5)	C(1)—O(1)	1.16(7)
Rh(4)—Rh(5)	2.754(5)	C(2)—O(2)	1.19(7)
Rh(4)—Rh(6)	2.762(5)	C(3)—O(3)	1.12(7)
Rh(5)—Rh(6)	2.707(5)	C(4)—O(4)	1.11(7)
		C(5)—O(5)	1.15(7)
Ni—C(5)	1.62(6)	C(6)—O(6)	1.27(8)
Rh(1)—C(10)	1.87(5)	C(7)—O(7)	1.14(8)
Rh(2)—C(8)	1.77(5)	C(8)—O(8)	1.19(7)
Rh(3)—C(12)	1.91(5)	C(9)—O(9)	1.19(7)
Rh(4)—C(7)	1.85(5)	C(10)—O(10)	1.15(7)
Rh(5)—C(16)	1.60(5)	C(11)—O(11)	1.24(7)
Rh(6)—C(11)	1.71(5)	C(12)—O(12)	1.16(7)
		C(13)—O(13)	1.17(7)
		C(14)—O(14)	1.16(7)
Ni—C(4)	1.96(7)	C(15)—O(15)	1.16(7)
Ni—C(14)	1.96(6)	C(16)—O(16)	1.22(7)
Ni—C(15)	2.04(7)		
Rh(1)—C(4)	1.94(5)	⟨C—C⟩ [a]	1.53(9)
Rh(2)—C(15)	1.91(5)	⟨C—N⟩ [a]	1.45(8)
Rh(3)—C(9)	1.98(5)		
Rh(3)—C(13)	1.94(5)		
Rh(4)—C(14)	1.95(5)		
Rh(5)—C(13)	1.97(5)		
Rh(6)—C(6)	1.88(5)		
Rh(6)—C(9)	2.02(5)		
Rh(5)—C(6)	1.84(5)		

[a] Average values for the TBA^+ cation.

counts (10 s each) at both sides of the peak were averaged. Three standard reflections were measured every 90 minutes to check the experimental conditions and the decay of the crystal; no significant variations were detected.

The data were corrected for Lorentz and polarization factors and for absorption $\mu = 27.25$ (cm^{-1}) using an azimuthal scan of three general reflections.

8312 independent reflections were collected, of which 3232 were considered as observed having net intensities $I \geqslant 3\sigma(I)$.

The structure was solved by Patterson and Fourier methods and refined by block diagonal least square using anisotropic temperature factors for Rh and Ni atoms and isotropic for the other nonhydrogen atoms.

The final agreement factor $R = \Sigma(|F_o| - K|F_c|)/\Sigma|F_o|$ was 0.069 for the observed reflections.

The scattering factors from ref. 9 were used, including corrections for the

TABLE 3

RELEVANT BOND ANGLES (°)
(e.s.d.'s on the last significant digit are given in parentheses)

Ni—Rh(1)—Rh(2)	58.6(3)		
Ni—Rh(2)—Rh(1)	58.4(3)		
Ni—Rh(2)—Rh(4)	58.4(3)		
Ni—Rh(4)—Rh(1)	58.4(3)		
Ni—Rh(4)—Rh(2)	58.7(2)		
Ni—Rh(1)—Rh(4)	58.4(3)		
Rh(1)—Rh(3)—Rh(6)	61.2(1)		
Rh(1)—Rh(6)—Rh(3)	60.8(1)	Rh(2)—Rh(3)—Rh(6)	90.6(1)
Rh(1)—Rh(2)—Rh(3)	60.1(1)	Rh(2)—Rh(4)—Rh(6)	90.3(1)
Rh(1)—Rh(3)—Rh(2)	59.4(2)	Rh(3)—Rh(2)—Rh(4)	88.9(1)
Rh(1)—Rh(2)—Rh(4)	59.9(1)	Rh(3)—Rh(6)—Rh(4)	90.4(1)
Rh(1)—Rh(4)—Rh(2)	60.1(2)		
Rh(1)—Rh(4)—Rh(6)	60.9(1)	Ni—C(5)—O(5)	171.7(9)
Rh(1)—Rh(6)—Rh(4)	59.5(1)	Rh(1)—C(10)—O(10)	176.8(8)
Rh(1)—Ni—Rh(2)	63.0(1)	Rh(2)—C(8)—O(8)	167.4(8)
		Rh(3)—C(12)—O(12)	145.0(8)
Rh(1)—Ni—Rh(4)	63.0(1)	Rh(4)—C(7)—O(7)	171.7(8)
		Rh(5)—C(16)—O(16)	146.0(8)
		Rh(6)—C(11)—O(11)	179.6(8)
Rh(2)—Rh(1)—Rh(3)	60.4(1)		
Rh(2)—Rh(1)—Rh(4)	59.9(1)	Ni—C(4)—Rh(1)	85.3(8)
Rh(2)—Rh(3)—Rh(5)	60.8(1)	Ni—C(14)—Rh(4)	84.8(9)
Rh(2)—Rh(5)—Rh(3)	60.8(1)	Ni—C(15)—Rh(2)	83.9(9)
Rh(2)—Rh(4)—Rh(5)	60.9(2)	Ni—C(14)—O(14)	134.0(9)
Rh(2)—Rh(5)—Rh(4)	59.6(1)	Ni—C(4)—O(4)	128.9(8)
		Ni—C(15)—O(15)	129.0(9)
Rh(2)—Ni—Rh(4)	62.9(1)	Rh(3)—C(9)—Rh(6)	85.5(8)
		Rh(3)—C(9)—O(9)	140.3(8)
		Rh(6)—C(9)—O(9)	133.9(8)
Rh(3)—Rh(1)—Rh(6)	58.2(1)	Rh(3)—C(13)—Rh(5)	88.4(8)
Rh(3)—Rh(5)—Rh(6)	59.9(1)	Rh(3)—C(13)—O(13)	136.1(8)
Rh(3)—Rh(6)—Rh(5)	60.4(1)	Rh(5)—C(13)—O(13)	135.4(8)
Rh(3)—Rh(2)—Rh(5)	58.4(1)	Rh(5)—C(6)—Rh(6)	93.2(8)
		Rh(5)—C(6)—O(6)	133.9(8)
Rh(4)—Rh(1)—Rh(6)	59.6(2)	Rh(6)—C(6)—O(6)	132.8(8)
Rh(4)—Rh(2)—Rh(5)	59.4(1)		
Rh(4)—Rh(6)—Rh(5)	60.5(2)		
Rh(4)—Rh(5)—Rh(6)	60.8(1)		
Rh(5)—Rh(3)—Rh(6)	59.7(1)		
Rh(1)—C(1)—Rh(2)	79.9(6)		
Rh(1)—C(1)—Rh(3)	76.5(7)		
Rh(3)—C(1)—Rh(2)	78.1(6)		
Rh(1)—C(3)—Rh(4)	79.8(6)		
Rh(1)—C(3)—Rh(6)	77.1(7)		
Rh(4)—C(3)—Rh(6)	76.0(6)		
Rh(2)—C(2)—Rh(4)	81.2(6)		
Rh(2)—C(2)—Rh(5)	80.4(6)		
Rh(4)—C(2)—Rh(5)	79.2(6)		
Rh(1)—C(1)—O(1)	131.5(8)		
Rh(2)—C(1)—O(1)	136.9(8)		
Rh(3)—C(1)—O(1)	131.0(9)		
Rh(1)—C(3)—O(3)	133.1(8)		
Rh(4)—C(3)—O(3)	137.6(8)		
Rh(6)—C(3)—O(3)	129.5(8)		
Rh(2)—C(2)—O(2)	131.7(8)		
Rh(4)—C(2)—O(2)	131.5(8)		
Rh(5)—C(2)—O(2)	132.4(8)		

real part of the anomalous dispersion for Rh and Ni.

The final positional and thermal parameters are listed in Table 1. Values of relevant bond lengths and angles are given in Tables 2 and 3. A list of F_o and F_c and a Table of atomic coordinates and thermal parameters for the $[N(n\text{-}Bu_4]^+$ cation may be obtained from the authors on request.

Acknowledgements

We thank the CNR for financial assistance and Dr. S. Martinengo for his interest in this work.

References

1 A. Fumagalli, S. Martinengo, P. Chini, A. Albinati, S. Brückner and B.T. Heaton, J. Chem. Soc. Chem. Comm., (1978) 195.
2 P. Chini, G. Longoni and V.G. Albano, Adv. Organometal. Chem., 14 (1976) 285.
3 S. Martinengo and P. Chini, Gazz. Chim. Ital., 102 (1972) 344.
4 G. Longoni, P. Chini and A. Cavalieri, Inorg. Chem., 15 (1976) 3025.
5 V.G. Albano, P.L. Bellon and G.F. Ciani, J. Chem. Soc. Chem. Commun., (1969) 1024.
6 A. Fumagalli, T.F. Koetzle, F. Takusagawa, P. Chini, S. Martinengo and B.T. Heaton; J. Amer. Chem. Soc., 102 (1980) 1740.
7 S. Martinengo, A. Fumagalli, P. Chini, V.G. Albano and C.F. Ciani, J. Organometal. Chem. 116 (1976) 333.
8 A. Fumagalli, S. Martinengo, P. Chini, A. Albinati and S. Brückner, presented at XIXth I.C.C.C. Prague, 1978, to be published.
9 International Tables for X-ray Crystallography, Vol. IV The Kynoch Press, Birmingham, 1976.